Discretized versus continuous models of p-wave interacting fermions in one dimension

Dominik Muth* and Michael Fleischhauer
Fachbereich Physik und Forschungszentrum OPTIMAS, Technische Universität Kaiserslautern, D-67663 Kaiserslautern, Germany

Bernd Schmidt
Institut für Theoretische Physik, Johann Wolfgang Goethe-Universität Frankfurt, D-60438 Frankfurt am Main, Germany
(Received 23 April 2010; published 6 July 2010)

We present a general mapping between continuous and lattice models of Bose and Fermi gases in one dimension, interacting via local two-body interactions. For s-wave interacting bosons we arrive at the Bose-Hubbard model in the weakly interacting, low-density regime. The dual problem of p-wave interacting fermions is mapped to the spin-1/2 XXZ model close to the critical point in the highly polarized regime. The mappings are shown to be optimal in the sense that they produce the least error possible for a given discretization length. As an application we examine the ground state of an interacting Fermi gas in a harmonic trap, calculating numerically real-space and momentum-space distributions as well as two-particle correlations. In the analytically known limits the convergence of the results of the lattice model with the continuous one is shown.

DOI: 10.1103/PhysRevA.82.013602 PACS number(s): 03.75.Hh, 05.30.Fk, 02.70.−c, 34.50.Cx

I. INTRODUCTION

Triggered by the recent successes in the experimental realization of strongly interacting atomic quantum gases in one spatial dimensional (1D) [1–5], there is increasing interest in the theoretical description of these systems beyond the mean-field level. Model Hamiltonians describing homogeneous 1D quantum gases with contact interaction are often integrable by means of the Bethe ansatz [6–9]. In practice, however, only a small number of quantities can actually be obtained from the Bethe ansatz or explicit calculations are restricted to a small number of particles. Properties associated with low-energy or long-wavelength excitations can, to very good approximation, be described by bosonization techniques [10]. For more general problems one has to rely on numerical techniques such as the density matrix renormalization group (DMRG) [11,12] or the related time-evolving block decimation (TEBD) [13,14]. Both were originally developed for lattice models, and thus to apply them to continuous systems requires a proper mapping between the true continuum model and a lattice approximation. In fact any numerical technique describing a continuous system relies on some sort of discretization. Here we consider massive bosonic or fermionic particles with contact interactions. Only two types of contact interaction potentials are allowed for identical, nonrelativistic particles, representing either bosons with s-wave interactions or fermions with p-wave interactions. Both systems are dual and can be mapped onto each other by the well-known boson-fermion mapping [15,16]. A proper discretization of 1D bosons with s-wave interaction is straightforward and has been used quite successfully to calculate ground-state [17], finite temperature [18], and dynamical problems [19] for trapped 1D gases. For p-wave interacting fermions a similar, straightforward discretization fails, however, as can be seen when comparing numerical results obtained using such a model with those obtained from the bosonic Hamiltonian after boson-fermion mapping. Using a general approach to quantum gases in 1D with contact interaction [20], we here derive a proper mapping between the continuous model and the lattice approximation. We show, in particular, that p-wave interacting fermions are mapped to the critical spin-1/2 XXZ model. By virtue of the boson-fermion mapping, the same can be done for s-wave interacting bosons, thus maintaining integrability in the map between continuous and discretized models. As an application we calculate the real-space and momentum-space densities of the ground state of a p-wave interacting Fermi gas in a harmonic trap, as well as local and nonlocal two-particle correlations in real space. To prove the validity of the discretized fermion model we compare the numerical results with those obtained from the dual-bosonic model as well as with Bethe ansatz solutions when available.

II. ONE-DIMENSIONAL QUANTUM GASES WITH GENERAL CONTACT INTERACTIONS

We here consider quantum gases, which are fully described by their two-particle Hamiltonian; that is, the Hamiltonian is a sum of the form

$$H = -\frac{1}{2}\sum_j \partial_{x_j}^2 + \sum_{i<j} V(x_i - x_j). \tag{1}$$

Additionally, we require that the true interaction potential can be approximated by a local pseudopotential; that is, it vanishes for $x_i \neq x_j$. Since we are in one dimension, this leads to the exact integrability of these models in the case of translational invariance [7] using the coordinate Bethe ansatz [6,9].

For deriving a discretized Hamiltonian, it is sufficient to consider the relative wave function $\phi(x = x_1 - x_2)$ of just *two* particles. The Hamiltonian then reads

$$H = -\partial_x^2 + V(x), \tag{2}$$

where we have dropped the term corresponding to the freely evolving center of mass.

The continuous two-particle case has been analyzed by Cheon and Shigehara [16,21]. The local pseudopotential V is fully described by a boundary condition on ϕ at $x = 0$: Since ϕ fulfills the free Schrödinger equation away from 0, it must

*muth@physik.uni-kl.de

have a discontinuity at the origin as an effect of the interaction. Thus we see that

$$\partial_x^2\phi(x) = \begin{cases} \phi''(x), & x \neq 0, \\ \delta(x)[\phi'(0^+) - \phi'(0^-)] & \\ \quad + \delta'(x)[\phi(0^+) - \phi(0^-)] & x = 0. \end{cases} \tag{3}$$

In the case of distinguishable or spinful [22] particles, both singular terms contribute. Due to symmetry, the term proportional to the δ function can only be nonzero for bosons, while the δ' term exists only for fermions. That is, for bosons we have

$$\partial_x^2\phi(x) = \begin{cases} \phi''(x), & x \neq 0 \\ 2\delta(x)\phi'(0), & x = 0, \end{cases} \tag{4}$$

and for fermions,

$$\partial_x^2\phi(x) = \begin{cases} \phi''(x), & x \neq 0 \\ 2\delta'(x)\phi(0), & x = 0. \end{cases} \tag{5}$$

To get proper eigenstates (i.e., without any singular contribution), the pseudopotential V acting on the wave function must absorb the singular contributions from the kinetic energy. Thus the only possible form of a local pseudopotential for bosons is $V_B\phi = g_B\delta(x)\phi(0)$, while that for fermions reads $V_F\phi = -g_F\delta'(x)\phi'(0)$. Note that ϕ (ϕ') is continuous at 0 for bosons (fermions). These two possibilities represent the well-known cases where the particles interact either by s-wave scattering only or by p-wave scattering only, and the interaction strength corresponds to the scattering length or scattering volume, respectively, which are the only free parameters left.

Since all wave functions must have the respective symmetry, we can restrict ourselves in the following to the $x > 0$ sector. We write $\phi(0)$ for $\lim_{x\to 0^+}\phi(x)$ and $\phi'(0)$ for $\lim_{x\to 0^+}\phi'(x)$. The preceding shows that V imposes a boundary condition on every proper wave function:

$$\begin{aligned} \phi'(0) &= \frac{g_B}{2}\phi(0) \quad \text{for bosons,} \\ \phi'(0) &= -\frac{2}{g_F}\phi(0) \quad \text{for fermions.} \end{aligned} \tag{6}$$

Equations (3) and (6) reveal a one-to-one mapping between the two cases; that is, every solution for the bosonic problem yields a solution for the fermionic problem with $g_B = -4/g_F$ by symmetrizing the wave function, and vice versa.

At this point we emphasize that boundary conditions of the form of Eqs. (6) are the only ones that are equivalent to a local potential [21,23]. While boundary conditions involving higher order derivatives can be taken into account to describe experimental realizations using cold gases in quasi-1D traps [24], they necessarily require finite-range potentials and cannot be described fully by local pseudopotentials.

III. DISCRETIZATION

The treatment of continuous gases in 1D using numerical techniques requires proper discretization. That is, we approximate the two-particle wave function $\phi(x) \in L^2(\mathbb{R})$ by a complex number $\phi_j \in \ell^2(\mathbb{Z})$, where the integer index j describes the discretized relative coordinate $x = x_1 - x_2$. We interpret $|\phi_j^2|$ as the probability of finding the two particles between $(j - \frac{1}{2})\Delta x$ and $(j + \frac{1}{2})\Delta x$. To apply numerical methods such as DMRG or TEBD [13,14] efficiently, it is favorable to have local or, at most, nearest-neighbor interactions in the lattice approximation of the continuous model. It will turn out that the preceding systems can all be discretized using such nearest-neighbor interactions only.

We start with the kinetic term, which can be approximated by

$$\partial_x^2 \mapsto \frac{\phi_{j-1} - 2\phi_j + \phi_{j+1}}{\Delta x^2}. \tag{7}$$

In what follows, we derive two distinct discretizations: first for the bosons, where we allow for double-occupied lattice sites and can therefore use on-site interactions to reproduce the boundary conditions (6), and then for fermions, where double occupation is forbidden by the Pauli principle and interactions between neighbors are necessary in the lattice model. Note, however, that both descriptions are equivalent due to the Bose-Fermi mapping in the continuum limit.

A. Bosonic mapping

In the lattice approximation the kinetic-energy term, Eq. (3) reads

$$\partial_x^2\phi(x) = \begin{cases} \frac{\phi_{j-1}-2\phi_j+\phi_{j+1}}{\Delta x^2}, & j > 0, \\ \frac{2(\phi_1-\phi_0)}{\Delta x^2}, & j = 0. \end{cases} \tag{8}$$

Thus assuming a local contact interaction only, we find for the bosons

$$(H\phi)_j = \begin{cases} -\frac{\phi_{j-1}-2\phi_j+\phi_{j+1}}{\Delta x^2}, & j > 0, \\ U\phi_0 - \frac{2\phi_1-2\phi_0}{\Delta x^2}, & j = 0. \end{cases} \tag{9}$$

To determine the value of U, we assume that it can be expressed as a series in Δx and evaluate the stationary Schrödinger equation $(H\phi)_j - E\phi_j = 0$ at $j = 0$. Re-expressing ϕ_1 in terms of $\phi(0)$ by means of the discretized version of the contact condition (6),

$$\phi_1 = \phi(0) + \Delta x \underbrace{\phi'(0)}_{=\frac{g_B}{2}\phi(0)} + \frac{\Delta x^2}{2}\underbrace{\phi''(0)}_{=-E\phi(0)} + \cdots, \tag{10}$$

we arrive at

$$\begin{aligned} 0 &= (H\phi)_{j=0} - E\phi_{j=0} \\ &= U\phi(0) + \frac{2\phi(0)}{\Delta x^2} - E\phi(0) - \frac{2}{\Delta x^2} \\ &\quad \times \left[\phi(0) + \Delta x\frac{g_B}{2}\phi(0) - \frac{1}{2}\Delta x^2 E\phi(0) + \mathcal{O}(\Delta x^3)\right]. \end{aligned} \tag{11}$$

Equating orders gives

$$U = \frac{g_B}{\Delta x} + \mathcal{O}(\Delta x). \tag{12}$$

The constant term vanishes, since $-\partial_x^2\phi = E\phi$ for any eigenstate. The higher orders $\mathcal{O}(\Delta x)$ contain E and would thus not be independent on the eigenvalue. This is perfectly consistent, since discretizations will only work as long as the lattice spacing is much smaller than all relevant (wave) lengths in the system. Thus the lowest order in (12) is already optimal.

There are no higher order corrections possible for a general state.

We can now easily write down the corresponding *many*-particle Hamiltonian for the case of indistinguishable bosons in *absolute* coordinates, represented by an integer index i, and in second quantization,

$$H = \sum_i \left[-J(a_i^\dagger a_{i+1} + \text{H.a.}) + \frac{U}{2} a_i^\dagger a_i^\dagger a_i a_i + V_i a_i^\dagger a_i \right]. \tag{13}$$

Here a_i is the bosonic annihilator at site i and V_i introduces an additional external potential in the obvious way. So, not surprisingly, we have arrived at the Bose-Hubbard Hamiltonian as a lattice approximation to 1D bosons with s-wave interaction. Since Δx must be smaller than all relevant length scales, however, in the low-filling and weak-interaction limits, $U \ll J = \frac{1}{2\Delta x^2}$.[1] This, of course, does not imply that the corresponding Lieb-Liniger gas is in the weakly interacting regime. This result might seem trivial, since we can also get it directly by substituting the field operator in the continuous model: $\Psi(j\Delta x) \mapsto \frac{a_j}{\sqrt{\Delta x}}$ [17]. However, this simple and naive discretization does not work in the fermionic case we are going to discuss now.

B. Fermionic mapping

For fermions the kinetic-energy term, Eq. (3), in lattice approximation reads

$$\partial_x^2 \phi(x) = \begin{cases} \frac{\phi_{j-1} - 2\phi_j + \phi_{j+1}}{\Delta x^2}, & j > 1, \\ \frac{\phi_2 - 2\phi_1}{\Delta x^2}, & j = 1, \\ 0, & j = 0. \end{cases} \tag{14}$$

Due to the antisymmetry of the wave function, ϕ_0 must vanish; that is, the simplest way interactions come into the lattice model is for nearest neighbors. Thus for the Hamiltonian we write

$$(H\phi)_j = \begin{cases} -\frac{\phi_{j-1} - 2\phi_j + \phi_{j+1}}{\Delta x^2}, & j > 1, \\ B\phi_1 - \frac{\phi_2 - 2\phi_1}{\Delta x^2}, & j = 1, \\ 0, & j = 0. \end{cases} \tag{15}$$

To obtain the value of B we proceed as in the case of bosons. As will be seen later it is most convenient to expand B in a series in the following way:

$$\frac{1}{B} = \Delta x^2 [B^{(2)} + \Delta x B^{(3)} + \mathcal{O}(\Delta x^2)]. \tag{16}$$

Now the stationary Schrödinger equation for $j = 1$ yields

$$0 = 1 - \frac{2}{g_F}\Delta x - \frac{\Delta x^2}{2} E + \mathcal{O}(\Delta x^3) + (B^{(2)} + \Delta x B^{(3)} + \Delta x^2 B^{(4)} + \mathcal{O}(\Delta x^2))[1 + \mathcal{O}(\Delta x^3)]. \tag{17}$$

Equating orders results in

$$B^{(2)} = -1, \quad B^{(3)} = \frac{2}{g_F}, \quad B^{(4)} = \frac{1}{2} E. \tag{18}$$

Note that this time the interaction appears only in the *second* lowest order, which cannot be described by a simple substitution formula. The next higher order contained in $\mathcal{O}(\Delta x^2)$ does not vanish but, again, depends on the energy as expected. If we had chosen a straightforward expansion of B instead of (16), the next order after the one that introduces the interaction would again have contained the interaction parameter:

$$B = -\frac{1}{\Delta x^2} - \frac{2}{g_F \Delta x} - \frac{4}{g_F^2} + \frac{E}{2} + \mathcal{O}(\Delta x). \tag{19}$$

Neglecting this term would therefore introduce a larger error than in the chosen expansion (16). In fact, the low-energy scattering properties would be reproduced only to 1 order less. For the bosons this problem did not occur (12). From (16) we read that the optimal result in the fermionic case is

$$B = -\frac{1}{\Delta x^2} \left(\frac{1}{1 - \frac{2\Delta x}{g_F}} \right). \tag{20}$$

The corresponding many-body Hamiltonian for indistinguishable fermions reads

$$H = \sum_i [-J(c_i^\dagger c_{i+1} + \text{H.a.}) + B c_i^\dagger c_i c_{i+1}^\dagger c_{i+1} + V_i c_i^\dagger c_i^\dagger], \tag{21}$$

where now c_i is a fermionic annihilator at site i. Equation (21) describes spin-polarized lattice fermions with hopping J and nearest-neighbor interaction B. In contrast to the bosonic case, Eq. (18), where the correct discretized model can be obtained from the continuum Hamiltonian just by setting $\Psi(x) \to a_i/\sqrt{\Delta x}$, we now see from (20) and (21) that a similar naive and straightforward discretization fails in the case of p-wave interacting fermions.

The failure of a naive discretization of the fermionic Hamiltonian becomes transparent if we map this model to that of a spin lattice: Using the Jordan-Wigner transformation,

$$\sigma_i^+ = \exp\left\{ i\pi \sum_{l<i} c_l^\dagger c_l \right\} c_i, \quad \sigma_i^z = 2c_i^\dagger c_i - 1, \tag{22}$$

(21) can be mapped to the spin-1/2 XXZ model in an external magnetic field,

$$H = \sum_i \left\{ -\frac{1}{4\Delta x^2} \left(\sigma_i^x \sigma_{i+1}^x + \sigma_i^y \sigma_{i+1}^y + \Delta(\sigma_i^z + 1)(\sigma_{i+1}^z + 1) \right) + V_i \sigma_i^z \right\}, \tag{23}$$

where the anisotropy parameter defining the XXZ model is $\Delta = -1/[1 - \frac{2\Delta x}{g_F}]$.

There is an easy way to see that these mappings are quite physical by considering the ground states: The repulsive Bose gas ($g_B > 0$) maps to the repulsive ($U > 0$) Bose-Hubbard model in the superfluid, low-filling regime, which has an obviously gaslike ground state. The same is true for the corresponding attractively interacting ($g_F < 0$) Fermi gas, which maps to the ferromagnetic XXZ model, which, due to

[1] In the case of ground-state calculations as done in Sec. IV we actually achieve good results even before J exceeds U. However, for nonequilibrium dynamics [19] it can become crucial that the bandwidth proportional to J is large compared to the pairing energy U.

the specific form of the interaction parameter in the discretized fermion model, Eq. (20), is always in the critical regime close to the transition point ($\Delta \xrightarrow{\Delta x \to 0} -1^+$). A naive discretization would have led to an anisotropy parameter that could cross the border to the gapped phase, which is clearly unphysical.

In the attractive Bose gas, bound states emerge, which lead to a collapse of the ground state, as is, of course, also true in the Bose-Hubbard model for $U < 0$. On the fermionic side, this collapse can also be observed, as for $\Delta < -1$, the XXZ model has a ferromagnetically ordered ground state, which leads to phase separation in the case of fixed magnetization.

Note that we call the Fermi gas repulsively interacting if $g_F > 0$, although B is negative in this case as well, and although there exist bound states, whose binding energy actually diverges as $g_F \to 0^+$, as is immediately clear from the Bose-Fermi mapping in the continuous case.

IV. INTERACTING FERMI GAS IN A HARMONIC TRAP

We now apply our method to the interacting Fermi gas in a harmonic trap:

$$H = -\frac{1}{2}\sum_{i=1}^{N}\partial_{x_i}^2 - \frac{g_F}{2}\sum_{j<i}\delta'(x_j - x_i)\,(\partial_{x_j} - \partial_{x_i})|_{x_j = x_i +} + \sum_{i=1}^{N}\frac{1}{2}x_i^2. \tag{24}$$

We here chose the trap length to set the length scale. The choice of an harmonic potential is arbitrary. We can include any other potential as well; the only crucial thing is that the potential should not have structures that remain unresolved within the chosen discretization length Δx. One can also consider a finite system, which then corresponds to an infinite box potential.

For $g_F = -\infty$ the system is called a fermionic Tonks-Girardeau gas [15,26,27]. It can be treated analytically, since it maps to free bosons under the Bose-Fermi mapping. For example, the momentum distribution is known for arbitrary particle numbers [25]. It is of special experimental relevance, since it is equivalent to the density distribution measured in a time-of-flight experiment. However, for an intermediate interaction strength numerical calculations are required. Those have been done so far only for small particle numbers and without arbitrary potentials, such that the Bethe ansatz can be used directly [28].

First, we note that we now have two options for discretizing the model. Direct discretization will yield the XXZ Hamiltonian, while Bose-Fermi mapping will result in the Bose-Hubbard Hamiltonian. Both methods, of course, have to produce exactly the same results.

Figure 1 shows the spatial density distribution in the ground state for $N = 25$ particles, that is,

$$\rho(x) = \int dx_2 \cdots dx_N |\phi(x, x_2, \ldots, x_N)|, \tag{25}$$

which is approximated by the discretized system as the diagonal elements of $\langle a_i^\dagger a_j \rangle$. The ground state of the discretized system is calculated using a TEBD code and an imaginary time evolution, which has already been applied successfully to calculate the phase diagram of a disordered Bose-Hubbard model [29]. The interaction strength is varied all the way from

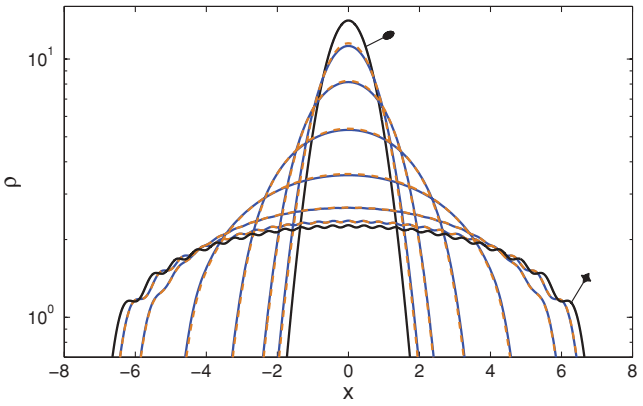

FIG. 1. (Color online) Local density distribution of the interacting Fermi or Bose gas. The dashed (orange) lines show results obtained by Bose-Fermi mapping and solving of the Bose-Hubbard lattice model; the solid (blue) lines correspond to the XXZ discretization. The interaction strength g_F is -51.2, -12.8, -3.2, -0.8, -0.2, and -0.05 from the narrow to the broad distributions. The solid black lines show the limiting cases of free fermions (broad; marked with a star) and infinitely strong interacting fermions (narrow; marked with an ellipse; corresponds to free bosons). Calculations were done for $\Delta x = \frac{1}{64}$. One can recognize the perfect agreement between the fermionic and the bosonic discretization approaches. Note that both fermions and bosons with corresponding interaction show the same local density, since the quantity is invariant under the Bose-Fermi mapping.

the free fermion regime to the regime of the fermionic Tonks-Girardeau gas. The density distribution changes accordingly from the profile of the free fermions, showing characteristic Friedel oscillations, to a narrow Gaussian peak for the fermionic Tonks-Girardeau gas. Note that the Bose-Fermi mapping does not affect the local density, so the curves are the same for the corresponding bosonic system. That is, the density distribution in the fermionic Tonks-Girardeau regime is identical to that of a condensate of noninteracting bosons. The curves obtained from the bosonic and fermionic lattice models are virtually indistinguishable, which shows that both approaches are consistent.

The corresponding momentum distribution for the fermions,

$$\rho_k(k) = \int dk_2 \cdots dk_N |\phi(k, k_2, \ldots, k_N)|, \tag{26}$$

which is quite different from that of the bosons, is shown in Fig. 2. It was obtained from the discretized wave function as the diagonal elements of the Fourier transform of $\langle a_i^\dagger a_j \rangle$. Again, perfect agreement between the bosonic and the fermionic lattice approximations is seen. In accordance with physical intuition invoking the uncertainty relation and Pauli principle, the momentum distribution broadens as the real-space distribution narrows. While for free particles, the real and momentum space descriptions coincide for the harmonic oscillator, the Friedel oscillations are deformed gradually toward the result for the fermionic Tonks-Girardeau gas calculated, for example, by Bender *et al.* [25]. The oscillations that remain in this limit are effects from the finite number of particles. They vanish as $1/N$, as can be seen from a Taylor expansion in $1/N$ of the expressions given in [25] for the Fermi-Tonks case.

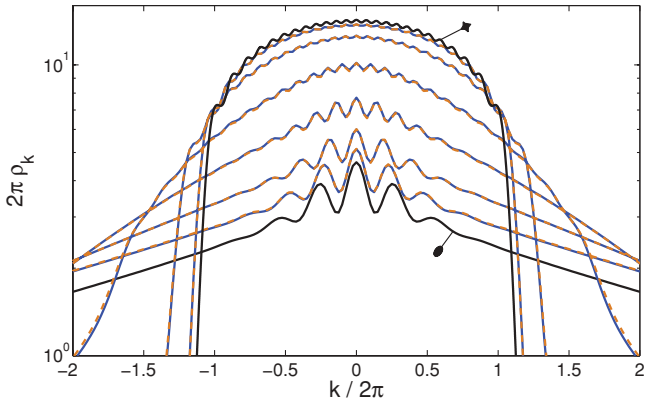

FIG. 2. (Color online) Momentum distribution of the interacting Fermi gas. Dashed (orange) lines show results via the Bose-Hubbard discretization; solid (blue) lines correspond to the XXZ discretization. The interaction strength g_F is -51.2, -12.8, -3.2, -0.8, -0.2, and -0.05 from the broad to the narrow distributions. Solid (black) lines show the limiting cases of free fermions (narrow; marked with a star) and infinitely strong interacting fermions (broad; marked with an ellipse; calculated from the formula given in [25]). Calculations were done for $\Delta x = \frac{1}{64}$. Again, there is perfect agreement between bosonic and fermionic discretization.

In Fig. 3 we have plotted the complete single-particle density matrix,

$$\rho(x,y) = \int dx_2 \cdots dx_N \phi^*(x,x_2,\ldots)\phi(y,x_2,\ldots), \qquad (27)$$

for different interaction strengths, starting from the Fermi-Tonks limit to the case of free fermions. One clearly recognizes two small off-diagonal peaks for greater interaction strengths. The weight of these peaks, which are responsible for the oscillations in the momentum distribution (Fig. 2), to the remaining part near the diagonal is $\frac{1}{N}$, as can be seen by

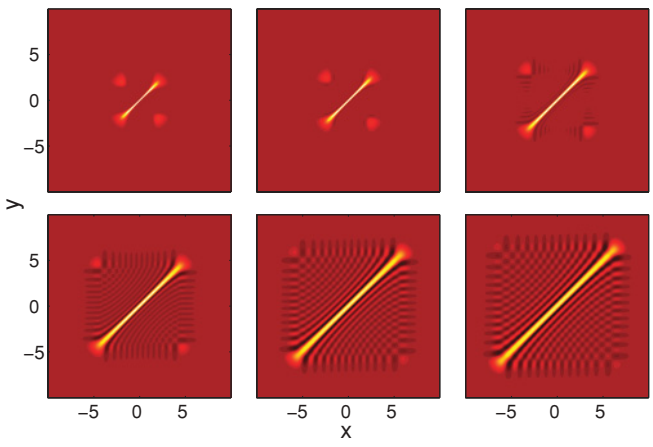

FIG. 3. (Color online) Single-particle density matrix of the interacting Fermi gas calculated using XXZ discretization. Light regions are positive; dark regions, negative. The interaction strength g_F is -51.2, -12.8, and -3.2 (top row) and -0.8, -0.2, and -0.05 (bottom row). Remember that the cloud size is independent of the particle number toward the fermionic Tonks limit (because there is condensation in the bosonic picture), while it grows as $\sqrt{N}$ for free fermions.

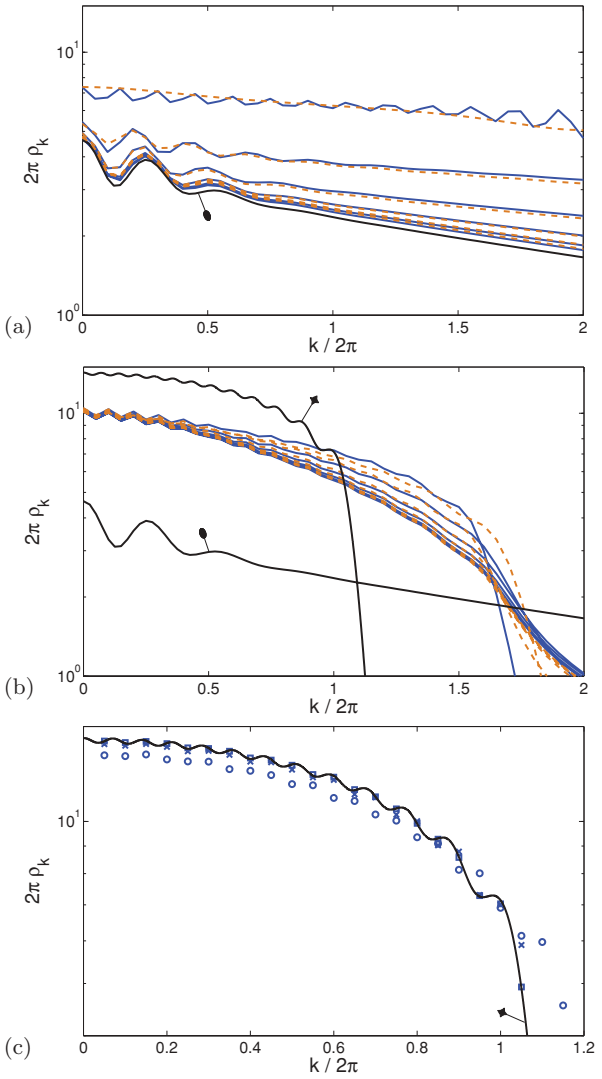

FIG. 4. (Color online) Momentum space distribution of the Fermi gas showing convergence of the method with discretization for (a) the Fermi-Tonks limit, (b) $g_F = -0.8$, and (c) the free fermionic case. Again, in (a) and (b) dashed (orange) lines show results via the Bose-Hubbard discretization, and solid (blue) lines correspond to XXZ discretization. (a) Results are shown for $\Delta x = \frac{1}{4}$, $\frac{1}{8}$, $\frac{1}{16}$, $\frac{1}{32}$, $\frac{1}{64}$, and $\frac{1}{128}$. As the grid gets finer, both discretization formulas converge to the exact result (black line; marked with an ellipse). (b) The same discretizations as in (a) were used, and again, there is convergence of both formulas toward a common limit, which, in this case, is not known analytically. Black lines are those shown in (a) and (c) and are for orientation. (c) Note that in this case there is no sense in distinguishing the two formulas, as implementing $U = \infty$ always means excluding double occupation of sites by bosons, which is immediately equivalent to simulating free fermions. We here show only $\Delta x = \frac{1}{4}$ (circles), $\frac{1}{8}$ (crosses), and $\frac{1}{128}$ (squares) to avoid confusion, since the lines converge quite quickly. Although the squares sit perfectly on top of the exact result (black line; marked with a star), they are not spaced densely enough to resolve the Friedel oscillations. This would require a lattice that extends across a region in space much larger than the N oscillator length where we have chosen to restrict the calculation to 20 oscillator lengths to speed it up.

analyzing the limiting case numerically, which can be done for much larger N also. The sign of the peaks is positive

only if N is odd and negative for even N, so the momentum distributions in Fig. 2 would show a minimum at $k = 0$ for all interaction strengths if N was chosen even instead of 25.

At first glance it may seem surprising that a mapping of a continuous, Bethe ansatz integrable Hamiltonian such as the Lieb-Liniger model to the nonintegrable Bose-Hubbard model should produce accurate results. However, since the Lieb-Liniger gas is dual to p-wave interacting fermions, as shown here its lattice approximation is equivalent to the spin-1/2 XXZ model, which is again Bethe ansatz integrable. Furthermore, full recovery of the properties of the continuous model can of course only be expected in the limit $\Delta x \to 0$. In Fig. 4 we show the momentum distribution of p-wave interacting fermions for decreasing discretization length Δx for three different values of the interaction strength. One clearly recognizes convergence of the results as $\Delta x \to 0$. In the two analytically tractable cases of a free fermion gas and the Fermi-Tonks gas, the curves quickly approach the exact ones.

As a final application we calculate the real-space two-particle correlations in a trap. The corresponding results are shown in Fig. 5. Again, the (blue) solid lines are obtained from the fermionic lattice model, and the dashed (orange) lines from the dual, bosonic model. Due to Pauli exclusion, $g^{(2)}(0) = 0$, and there is a pronounced dip in $g^{(2)}$ near the origin for noninteracting or weakly attractive fermions, while we again see Friedel oscillations for larger interparticle distances. In the dual, bosonic case the dip is enforced by a strong repulsive interaction. As the fermionic attraction is increased, the depth of this dip is decreased. There is a smooth transition to the perfect Gaussian shape expected for free bosons in the case of strongly interacting fermions.

Outside the point where the particle positions coincide, both discretization formulas give the same result. There is a discontinuity maintaining $g^{(2)}(0) = 0$ for the fermions, enforced by the symmetry of the wave functions. It should be noted that this singular jump is not reproduced in the dual, bosonic model. This is because the duality mapping of the discretized models is only valid for two particles at *different* lattice sites and the dual, bosonic model can only be used to calculate multiparticle correlations of fermions at pairwise different locations.

Finally, we note that using the discretization formulas (12) and (18), one can, of course, also calculate other many-body properties like of-diagonal order [27] using TEBD for larger systems. The method was also used to calculate out-of-equilibrium dynamics for bosonic gases in the repulsive [19] as well as the attractive regime [30]. A generalization to higher dimensions is not immediately evident and requires a separate discussion.

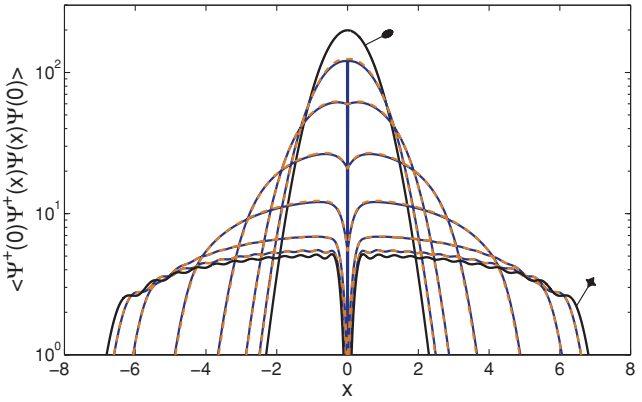

FIG. 5. (Color online) Density-density correlations of the interacting Fermi or Bose gas. Dashed (orange) lines show results obtained by Bose-Fermi mapping and solving of the Bose-Hubbard lattice model; solid (blue) lines correspond to the XXZ discretization. The interaction strength g_F is -51.2, -12.8, -3.2, -0.8, -0.2, and -0.05 from the narrow to the broad distributions. Solid black lines show the limiting cases of free fermions (broad; marked with a star) and infinitely strong interacting fermions (narrow; marked with an ellipse; corresponds to free bosons). Calculations were done for $\Delta x = \frac{1}{64}$. One can recognize the perfect agreement between the fermionic and the bosonic discretization approaches apart from $x = 0$ (see text). Note that both fermions and bosons with corresponding interaction show the same density-density correlations, since the quantity is invariant under the Bose-Fermi mapping.

The method presented in this paper is not limited to problems including only one species of particles. We can also describe fermions with spin degrees of freedom, mixtures of bosons and fermions, or even a gas with Boltzmann statistics. Whenever two distinguishable particles interact, both terms in (3) can contribute; that is,, one ends up with an s-wave as well as a p-wave contribution to the interaction. Following lines similar to those in this paper, one can then easily derive a corresponding Hamiltonian in second quantization.

ACKNOWLEDGMENTS

Special thanks go to Anna Minguzzi for stimulating discussions that led to this work. The authors would also like to thank Maxim Olshanii and Fabian Grusdt for valuable input. Finally, the financial support of the graduate school of excellence MAINZ/MATCOR and Sonderforschungsbereich TR49 is gratefully acknowledged.

[1] T. Kinoshita, T. Wenger, and D. S. Weiss, Science **305**, 1125 (2004).
[2] B. Paredes, A. Widera, V. Murg, O. Mandel, S. Fölling, I. Cirac, G. V. Shlyapnikov, T. W. Hänsch, and I. Bloch, Nature **429**, 277 (2004).
[3] K. Gunter, T. Stoferle, H. Moritz, M. Kohl, and T. Esslinger, Phys. Rev. Lett. **95**, 230401 (2005).
[4] S. Hofferberth, I. Lesanovsky, B. Fischer, T. Schumm, and J. Schmiedmayer, Nature **449**, 324 (2007).
[5] E. Haller, M. Gustavsson, M. J. Mark, J. G. Danzl, R. Hart, G. Pupillo, and H. C. Nägerl, Science **325**, 1224 (2009).
[6] H. Bethe, Z. Phys. **71**, 205 (1931).
[7] E. H. Lieb and W. Liniger, Phys. Rev. **130**, 1605 (1963).

[8] V. E. Korepin, N. M. Bogoliubov, and A. G. Izergin, *Quantum Inverse Scattering Method and Correlation Functions* (Cambridge University Press, Cambridge, 1993).
[9] M. Gaudin, *La Fonction d'Onde de Bethe* (Masson, Paris, 1983).
[10] T. Giamarchi, *Quantum Physics in One Dimension* (Oxford University Press, New York, 2003).
[11] S. R. White, Phys. Rev. Lett. **69**, 2863 (1992).
[12] U. Schollwöck, Rev. Mod. Phys. **77**, 259 (2005).
[13] G. Vidal, Phys. Rev. Lett. **91**, 147902 (2003).
[14] G. Vidal, Phys. Rev. Lett. **93**, 040502 (2004).
[15] M. Girardeau, J. Math. Phys. **1**, 516 (1960).
[16] T. Cheon and T. Shigehara, Phys. Rev. Lett. **82**, 2536 (1999).
[17] B. Schmidt and M. Fleischhauer, Phys. Rev. A **75**, 021601(R) (2007).
[18] B. Schmidt, L. I. Plimak, and M. Fleischhauer, Phys. Rev. A **71**, 041601(R) (2005).
[19] D. Muth, B. Schmidt, and M. Fleischhauer, e-print arXiv:0910.1749 (2009).
[20] B. Schmidt, Ph.D. thesis, Technische Universität Kaiserslautern, 2009.
[21] T. Cheon and T. Shigehara, Phys. Lett. A **243**, 111 (1998).
[22] M. D. Girardeau and M. Olshanii, Phys. Rev. A **70**, 023608 (2004).
[23] P. Seba, Czech. J. Phys. **36**, 667 (1986).
[24] A. Imambekov, A. A. Lukyanov, L. I. Glazman, and V. Gritsev, Phys. Rev. Lett. **104**, 040402 (2010).
[25] S. A. Bender, K. D. Erker, and B. E. Granger, Phys. Rev. Lett. **95**, 230404 (2005).
[26] M. D. Girardeau and A. Minguzzi, Phys. Rev. Lett. **96**, 080404 (2006).
[27] A. Minguzzi and M. D. Girardeau, Phys. Rev. A **73**, 063614 (2006).
[28] Y. Hao, Y. Zhang, and S. Chen, Phys. Rev. A **76**, 063601 (2007).
[29] D. Muth, A. Mering, and M. Fleischhauer, Phys. Rev. A **77**, 043618 (2008).
[30] D. Muth and M. Fleischhauer, e-print arXiv:1006.5312 (2010).